Deliverable 1

Testing Protocol and Material Specifications for Basalt Fiber Reinforced Polymer Bars

Contract Number BE694
FSU Project ID: 042878

Submitted to:

Florida Department of Transportation
Research Center
605 Suwannee Street
Tallahassee, Florida 32399-0450

Chase C. Knight, Ph.D
Project Manager
FDOT State Materials Office

FAMU-FSU Engineering

Prepared by:

Raphael Kampmann, Ph.D.
Principal Investigator
Youneng Tang, Ph.D.
Co-Principal Investigator
Srichand Telikapalli
Graduate Research Assistant

FAMU-FSU College of Engineering
Department of Civil and Environmental Engineering
2525 Pottsdamer Street
Tallahassee, FL 32310

25/03/2019

Contents

List of Figures

List of Tables

Chapter 1

Background

1.1 Introduction

This chapter provides an overview of the history of Basalt fiber and uses in the construction industry in the form of Basalt Fiber Reinforced Polymer (BFRP) reinforcement bars (rebars), from the raw material to the final rebar product. To provide context and to offer a comprehensive state-of-the-art review of the alternative rebar industry, general FRP rebar materials are reviewed because clear commonalities exist between the constituent materials and the production methods of the most common FRP materials (basalt, glass, carbon, aramid, etc.). However, this chapter is mostly focused on techniques and materials use for the production of BFRP rebars. To facilitate an initial overview, a typical basalt rock, sized fibers, and a BFRP rebar can be seen in Figure 1.1. Like all fiber reinforced polymer materials, BFRP rebars are composite products.

Figure 1.1: Basalt rock, fiber, and rebar

A French researcher Paul Dhé invented basalt fibers in the year 1923 (Dhé, 1923). Manufacturers did not concentrate on basalt fibers due to the production difficulties and because the manufacturing of glass fibers was more profitable (Faruk et al., 2017). But the research on basalt fibers was continued for military purposes in the former soviet union during the Cold War period (Jamshaid and Mishra, 2016). Research findings were3 released for the use of civilians in 1995 after the collapse of the soviet union in 1991. Due to the confidentiality of the research until 1995, the use of basalt fibers in the construction industry is a developing technology. Though BFRP rebars are believed to have a promising future in replacing traditional black steel (y de Caso et al., 2012), carbon FRP, and glass FRP, the durability of BFRP rebar in response to chemical attacks is still unknown. Because BFRP rebar is a recently developed technology, a study of long-term saline and alkaline durability of BFRP rebars has yet to be performed. Accordingly, a detailed literature review about

the individual constituent materials and their currently documented behavior is presented in this chapter.

1.2 Source Material for Fibers

To produce basalt fibers, the source material from which the fibers are manufactured must be thoroughly studied because the physical, and the mechanical properties of the rebar (end product) depends on the basalt rock (Singha, 2012). The physical, mechanical, and durability properties of the source material play a key role in the production as they determine the characteristics of the final fibers.

Basalt fibers are made from molten basalt rock, which is a fine-grained igneous rock. Igneous rocks are one of the three major classification of rocks, with the other two being sedimentary and metamorphic rocks and more than 90 % of all igneous rocks are basalt. Igneous rocks are classified into volcanic rocks and plutonic rocks (Best, 2003), dependent on the the exposure conditions during cooling and hardening. Volcanic rocks are formed when magma solidifies under the earth surface, while plutonic rocks are formed when the lava solidifies on the surface of the earth. Basalt rock is formed only from solidified lava (Singha, 2012); when magnesium-rich and iron-rich lava is exposed to a rapid cooling process, it forms into basalt rock. The melting temperature of basalt ranges from 1500 °C to 1700 °C (2732 °F to 3092 °F). Almost 80% of Basalts are made from two minerals, Plagioclase and Pyroxene. Plagioclase is a series of tectosilicate minerals within the feldspar group. Pyroxene (P_x) are a group of rock forming inosilicate minerals found in igneous and metamorphic rocks. Two of the main constituents of basalt are SiO_2 and Al_2O_3 (Militkỳ et al., 2002). Table 1.1 shows the composition of a typical basalt rock according to Militkỳ et al. (2002) and Deák and Czigány (2009). Because basalt is a mineral, the chemical composition of the core rock varies widely depending

Table 1.1: Typical Basalt components

	Content Wt %	
Constituent	Militky2002a	Deak2009a
SiO_2	43.3–47	42.43–55.69
Al_2O_3	11–13	14.21–17.97
Fe_2O_3	5	10.80–11.68
CaO	10–12	7.43–8.88
MgO	8–11	4.06–9.45
Na_2O	5	2.38–3.79
TiO_2	5	1.10–2.55
K_2O	5	1.06–2.33

on the place of origin. Basalts with a wide range of chemical composition is used in the manufacturing of stone castings, ties, and staple fibers (Singha, 2012). But the fibers used for civil engineering purposes, which are continuous basalt fibers (CBF), have to fall within a very narrow range of chemical composition to form a chemically durable and desirable final product (Vasil'eva et al., 2014; Tatarintseva et al., 2012b). Most fiber manufacturers around the world are using the Andesitic basalt rock with 50 % SiO_2 by weight (Novitskii and Efremov, 2013; Morozov et al., 2001). Basalt rock has to satisfy specific criteria to be accepted as a source for manufacture of continuous basalt fiber (Johannesson et al., 2017), and Table 1.2 lists the acceptance limits according to Stekloplastics (2014); Toni Schneider (2015); Kochergin et al. (2013), and www.bavoma.com. It can be seen in Table 1.2 that the limits according to Kochergin et al. (2013) have much wider ranges then the ones listed by others, because these limits are applicable to a large range of applications which includes,

Table 1.2: Limits for chemical composition of basalt for CBF production

	Content Wt %			
Oxide	Stekloplastics (2014)	Toni Schneider (2015)	www.bavoma.com	Kochergin et al. (2013)
SiO_2	50-54(48-56)	45-60	47.5-55.0	38-55
Al_2O_3	7.5-15.0	12-19	14-20	3-20
FeO-Fe_2O_3	7.0-15	5-15	7-13	2-18
MgO	3-7	3-7	3-8.5	1-24
TiO_2	0.1-2	0.1-2	0.2-2	–
NaO+K_{20}+CaO	0.1-18	–	2.5-7.5(Na+K)	–
CaO	–	6-12	7-11	17
MnO	–	–	< 0.25	0.3
SO_3	–	–	< 0.2	–

for example, slag wool. The limits specified in the first, second, and third columns are narrower and are used in manufacture of continuous basalt fiber. The combination of alkali (Na_2O+K_2O) and silica content in volcanic rock is used to classify them through total alkali silica (TAS), which can be seen in Figure 1.2. It is important to study alkali and silica content of the rock because the limiting states and purity of rock

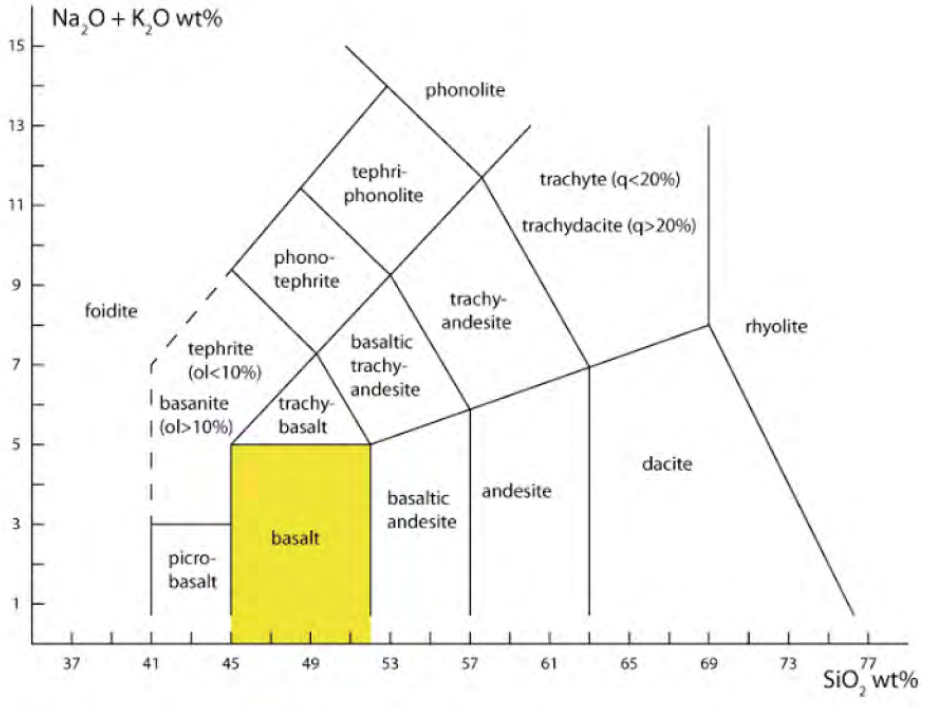

Figure 1.2: Total alkali silica

depends on the mineral composition. The most important properties of basalt rock to be analyzed before using it for the production of fibers are acidity modulus, viscosity modulus, and surface tension.

1.2.1 Acidity Modulus (M_a)

Acidity modulus is the most important parameter used in the manufacture of basalt fibers (Tatarintseva et al., 2012b,a). It is the ratio of acidic oxides to the basic oxides in the basalt rock as represented in equation 1.1.

$$M_a = \frac{SiO_2 + Al_2O_3}{CaO + MgO} \tag{1.1}$$

The equation relies on the weight percentage of the included oxides. If M_a is less than 1.2, the fibers are considered slag wool, which is very brittle with poor chemical durability (Johannesson et al., 2017; Kochergin et al., 2013). If the acidic modulus ranges from 1.2 to 1.5, the fibers are considered mineral wool, which is good for insulation purposes. But the mineral wool fibers are very brittle in nature. If M_a of the fibers is greater than 1.5, they are considered rock wool or basalt fiber. Table 1.3 lists the values of acidic modulus for different production forms. King et al. (2014) classified basalt rock based on SiO_2 content, and states

Table 1.3: Classification of acidity modulus (Johannesson et al., 2017)

References	Acidity Modulus (M_a)
Kochergin et al. (2013)	0.8-1.3 Slag
Singha (2012)	$<$ 1.2 Slag wool
	1.2-1.5 Mineral wool
	$>$ 1.5 Rock Wool, Basalt Fiber
Pisciotta et al. (2015)	$<$ 1.8 Mineral wool
	$>$ 1.8 Rock wool, Basalt fiber
Tatarintseva and Khodakova (2010)	$>$ 1.2 Staple and continuous fiber
	optimal for CBF

that the rock is considerably alkaline if SiO_2 is less than 42 %. Basalt rock is considered mildly acidic if SiO_2 % ranges between 43 % and 46 %, and acidic if SiO_2 is over 46 %.

1.2.2 Viscosity Modulus (M_v)

The viscosity modulus is defined as the ratio of the molar fractions of the acidic oxides to all other oxides. For the production of continuous fibers, Toni Schneider (2015) defined the limits of viscosity modulus to be 2 to 3. Pisciotta et al. (2015),Pico et al. (2011), and Perevozchikova et al. (2014) defined the viscosity modulus through Equation 1.2.

$$M_v = \frac{x_{SiO_2} + x_{Al_2O_3}}{2x_{Fe_2O_3} + x_{FeO} + x_{CaO} + x_{MgO} + x_{K_2O} + x_{Na_2O}} \tag{1.2}$$

In this equation, x is defined as the molar ratio of the oxides.

Viscosity (η)

To produce basalt fibers, the rock has to be melted down and the molten material requires a specific liquidity. The stiffness of the molten material is described by the viscosity. Viscosity is one of the properties that determines the suitability for the basalt in the production process of fibers. Based on empirical analysis, the viscosity range for molten basalt rock must be between 10 Pa to 30 Pa to form a continuous basalt fiber (Tatarintseva et al., 2012a; Tatarintseva and Khodakova, 2012; Dzhigiris et al., 1983). These limits

were derived from experimental analysis, and these limits were obtained at the melting temperatures ranging between 1300 °C and 1400 °C (Tatarintseva and Khodakova, 2012). The oxides that facilitate an increased viscosity (liquid stiffness) are Silica (SiO_2), Alumina (Al_2O_3), magnesium oxide (MgO), and trivalent iron (Fe_2O_3), while alkali metal oxides like potassium oxide (K_2O), sodium oxide (Na_2O), and divalent iron (FeO) contribute in decreasing the viscosity (Tatarintseva et al., 2012a). The viscosity of one particular basalt with composition shown in Table 1.4 can be calculated by using Equation 1.3 (Tatarintseva et al., 2012a).

$$\eta(T) = 3.26\left(\frac{\mathrm{SiO_2^{3.07}} + (\mathrm{FeO} + \mathrm{Fe_2O_3})^{1.34}}{\mathrm{Al_2O_3^{0.16}CaO^{0.4}}(T - 1100\,^{\circ}\mathrm{C})^{2.58}}\right)(M_a)^{1.25} \tag{1.3}$$

The oxides in this equation are supplied in weight percentage, T represents the temperature in °C, and the variables on the oxides are acidic modulus (M_a).

Table 1.4: Composition of basalt used in the viscosity equation (Tatarintseva et al., 2012a)

Oxide	Weight (%)
SiO_2	60.60
Al_2O_3	18.20
TiO_2	0.95
MnO	0.048
FeO+Fe_2O_3	7.2
MgO	2.20
Na_2O	2.30
K_{20}	3.45
P_2O_5	0.18
Other	4.70

Surface Tension (σ)

Surface tension is an important property, which must be determined in the production process of basalt fibers (Pisciotta et al., 2015). In continuous silicate fiber manufacture process, this property is known as fibreizability. The temperature at which the production process takes place depends on the ratio of the viscosity to the surface tension (η/σ). The stability of manufacturing process is directly proportional to this ratio. High modulus fibers are made from molten aluminosilicate glasses (Tatarintseva and Khodakova, 2012), and the η/σ ratio for these glasses is 100 Pa.

1.3 Fiber Types

This section describes the fiber types which are used in the manufacturing process of FRP rebars. Four major fiber types are used in FRP manufacturing: glass, basalt, carbon, and aramid fibers. Glass FRP are the predominantly used reinforced plastics in structural engineering due to the available research knowledge and low production cost. But, for engineering purposes, the mechanical properties of basalt FRP are comparatively better than the mechanical properties of glass FRP (Zych and Wojciech, 2012). Rebars made of other fibers are abundantly available in Asian countries (ACI Committee 440, 2007). A brief introduction to the four major fibers is given in the following subsections.

1.3.1 Carbon Fibers

Carbon fiber composites are fibers made from polyacrylonitrile (PAN) classified as high-modulus carbon fiber. Carbon fibers have the highest tensile strength and elastic modulus compared to other fibers. They have high resistance to alkali or acid attacks, and a high electrical conductivity. Carbon fibers are the most expensive fibers available in market (Nanni et al., 2014). Due to their high strength and elastic properties, they perform well in prestressing applications for bridge structures.

1.3.2 Aramid Fibers

Aramid fibers are polyamide-based fibers (Bagherpour, 2012), with Kevlar 29, 49 and 149 are the most predominantly used fiber grades for applications in structural engineering. Aramid fibers are in general strong in tension and have a higher elastic modulus in comparison to glass fibers (Bagherpour, 2012). They have higher resistance to fatigue and creep, the fibers are magnetically transparent and do not conduct electricity or heat. Due to its high resistance to heat, they are used for applications in furnaces. They are weak in high humid and chemical environments. Due to their high cost, these fibers are not widely used in construction (Nanni et al., 2014).

1.3.3 Glass Fibers

Glass fibers are the most common fibers used for structural applications, and specifically in bridge applications. The most common fibers are AR(Alkaline Resistant)-glass, E(Electrical)-glass, and S(High Strength)-glass. E-glass fibers are predominantly used in civil and industrial structures (Bagherpour, 2012). The glass fibers are highly resistant to moisture and have higher strength. The lime-alumina-borosilicate in sand is the major ingredient for the fiber manufacture (Bagherpour, 2012). S-glass is more expensive than E-glass and is less preferred by manufacturers. AR-glass does not have a proper sizing (see Section 1.6) compatibility for FRP manufacturing (Nanni et al., 2014). Unlike basalt fibers, the glass fiber manufacturing process includes additives like borax to achieve better chemical resistance (Aubourg et al., 1991). The major ingredient in the manufacturing of glass fibers is silica, while lime stone and soda ash are additives to lower the melting temperature.

1.3.4 Basalt Fibers

The concept of basalt fibers was first invented in the year 1953 at the Moscow Research Institute (Morova, 2013). The fibers were initially used in bulletproof vests for military purposes and the research was kept classified. Use of BFRP rebar in construction engineering has started after the collapse of the soviet union in the year 1991, when the research was allowed to be published for civilian use. Some manufacturers claim that the performance of basalt fibers is comparable to the performance of expensive carbon fibers and glass fibers (Singha, 2012). Similar to basalt rock, the basalt fibers are categorized based on the acidic modulus (M_a), and the acidic modulus is defined as the ratio of acidic to basic oxides. In the construction industry, basalt fibers with M_a ranging from 1.2 to 1.5 are used (Singha, 2012). In a direct comparison, basalt fibers have a higher elastic modulus than glass fibers. They have excellent heat resistance and perform well in heat intensive environments while also providing good acoustic damping (Singha, 2012). The density of the fibers are much lower ($2.8\,\frac{\mathrm{g}}{\mathrm{cm}^3}$) in comparison to steel. The moisture absorption of basalt fibers is approximately 1 % and they can withstand an alkaline environment with pH levels between 13 and 14. Although basalt fibers are less stable in strong acids, they retain 92 % and 75 % of their properties by only losing 5 % and 2 % of their weight when tested in 2(M) NaOH and 2(M) HCl, respectively (Singha, 2012).

1.3.5 Summary of Fiber Types

In this subsection, the typical mechanical, and physical properties of different fibers are summarized and compared. Important fiber properties according to Singha (2012) are shown in Table 1.5. The thermal properties of s-glass and basalt fibers are compared in Table 1.6 as determined by Singha (2012). It can be seen in that basalt fibers have better thermal properties in comparison to glass fibers. Table 1.7 lists mechanical properties of different fiber according to Nanni et al. (2014). The data in the table shows that basalt fibers have better mechanical properties in comparison to other fibers.

Table 1.5: Mechanical and physical properties of fibers (Singha, 2012)

		Fiber Type			
		Continuous Basalt	Carbon	Glass	
Properties	unit			E- glass	S- glass
Breaking Strength	MPa	3000 – 4840	3500 – 6000	3100 – 3800	4020 – 4650
Elastic Modulus	GPa	79.3 – 93.1	230 – 60	72.5 – 75.5	83 – 86
Breaking Extension	%	3.1	1.5 – 2.0	4.7	5.3
Fiber Diameter	µm	6 – 21	5 – 15	6 – 21	6 – 21
Linear Density	tex	60 – 4200	60 – 2400	40 – 4200	40 – 4200
Temperature Withstand	°C	−260 – 700	−50 – 700	−50 – 380	−50 – 380

Table 1.6: Thermal properties of fibers (Singha, 2012)

		Fiber Type	
Thermal Properties	unit	Basalt	E-glass
Maximum Operating Temperatures	°C	980	650
Sustained Operating Temperatures	°C	700	480
Minimum Operating Temperatures	°C	−2.6	−60
Thermal Conductivity	W/mK	0.031 – 0.038	0.034 – 0.04
Melting Temperature	°C	1280	1120
Thermal Expansion Coefficient	ppm/°C	8.0	5.4

Table 1.7: Typical mechanical properties of fibers (Nanni et al., 2014)

Type of Fiber	Density		Tensile strength		Tensile modulus		Tensile strain
	lb/yd^3	kg/m^3	ksi	N/mm^2	10^6 psi	10^6 N/m^2	%
Basalt	4720	2800	700	4827	12.9	88.95	3.1
E-glass	4215	2450	500	3448	10.5	72.40	2.4
S-glass	4215	2450	660	4550	12.4	85.50	3.3
AR-glass	3800	2250	260 - 500	1793 - 3448	10.1 - 11.0	69.64 - 75.85	2.0 - 3.0
High-modulus carbon	3290	1950	360 - 580	2482 - 4000	50.7 - 94.3	349.50 - 650.20	0.5
Low-modulus carbon	2950	1750	507	3496	34.8	239.90	1.1
Aramid (Kevlar 29)	2428	1440	400	2758	9.0	62.06	4.4
Aramid (Kevlar 49)	2428	1440	525	3620	18.0	124.11	2.2
Aramid (Kevlar 149)	2428	1440	500	3448	25.4	175.13	1.4

1.4 Basalt Fiber Production

The only raw ingredient used in the production process of basalt fibers is basalt rock (Zych and Wojciech, 2012), hence physical and mechanical properties of the fibers depend on the chemical composition of the rock. The basalt fibers are non-carcinogenic and non-toxic, and therefore, they are considered eco-friendly (Zych and Wojciech, 2012). Basalt fibers are made from molten basalt rock, which has a melting temperature of 1500 °C. Figure 1.3 depicts the production process of the basalt fiber, and it is shown that the crushed, washed basalt rock is transported to the furnace, first. Basalt rock absorbs the infrared energy, and therefore, it is kept in the smelter until it reaches a homogeneous temperature throughout the entire molten mass (Ipbüker et al., 2014). Molten basalt flows into the forehearth and is then forced through a platinum/rhodium crucible, which has a 9 µm to 24 µm opening, and continuous fibers are extracted. Starch, oil, gelatin, or wax is applied to the extracted fibers as sizing for fiber protection and to improve bond within the fiber-resin matrix (Bagherpour, 2012; Zych and Wojciech, 2012). The fibers are then shaped and stored in desired forms depending on specific final purpose (Pavlovski et al., 2007).

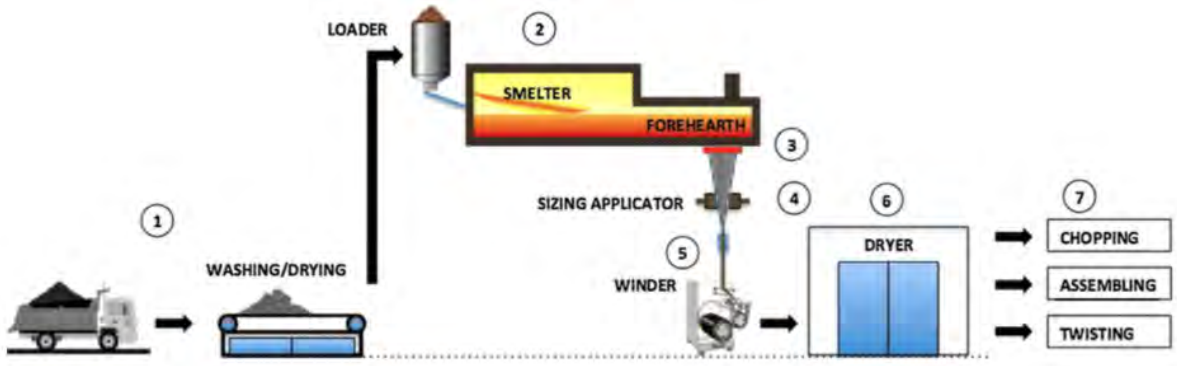

Figure 1.3: Basalt fiber production process (Ipbüker et al., 2014)

1.5 Chemical Durability Studies on Basalt Fibers

Ying and Zhou (2013) tested thermal stability of basalt, carbon and glass fibers in high temperature environments. The fibers were tested in tension after treating them with high temperatures (300 °C –600 °C). The corrosion properties of basalt fiber were also tested by Ying and Zhou (2013), for which the fibers were calcined at 300 °C for 3 h and 400 °C for 2 h before immersing them in water, acidic (hydrochloric acid) and alkali (sodium hydroxide) environments. The fibers were immersed for 24 h at 0 °C and 100 °C in all test solutions and weight retention of basalt fiber after 24 h immersion in boiling water, HCl (1mol/L), NaOH (1mol/L), NaOH (2mol/L) was 99 %, 97 %, 95 %, 92 %. The results of tensile strength of fibers after immersion period were plotted by (Ying and Zhou, 2013) and are shown in Figures 1.4, 1.5, and 1.6.

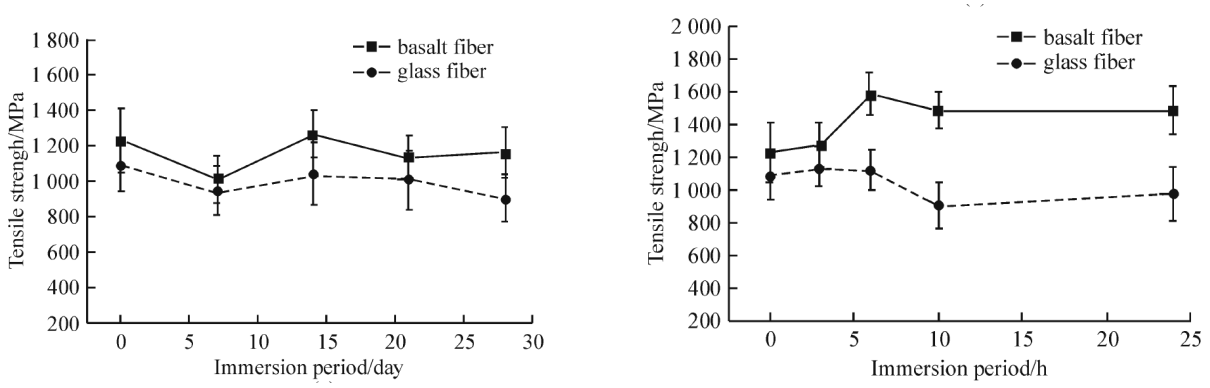

(a) Room temperature (b) 100 °C

Figure 1.4: Tensile strength retention of water treated fibers (up to 24 h)

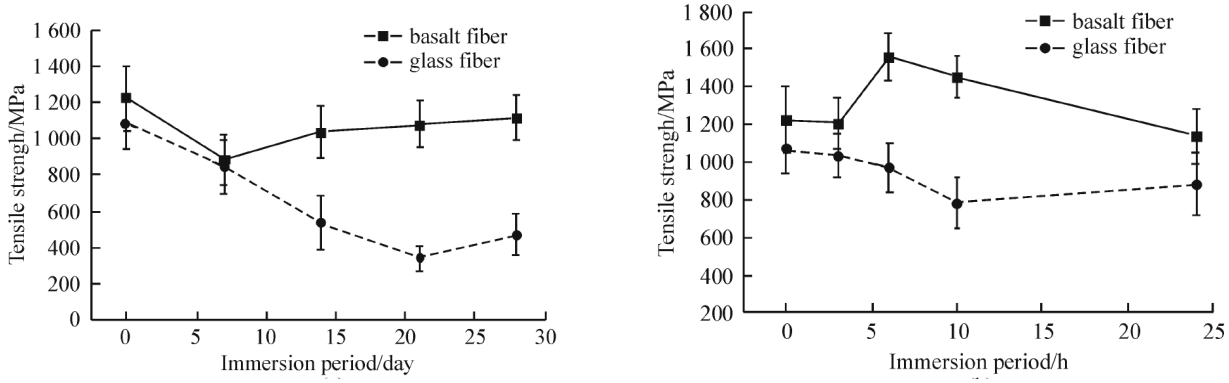

(a) Room temperature (b) 100 °C

Figure 1.5: Tensile strength of fibers in 1mol/L HCl for 24 h

Nasir et al. (2012) studied the corrosion behavior and the crack formation mechanism of basalt fiber in sulphuric acid and compared the result to the documented performance of E-glass fiber studied by Shokrieh et al. (2012). Nasir et al. (2012) kept the basalt fiber bundles in 5 % sulphuric acid for 720 h and tested the tensile strength of the fibers. The fibers were cleaned with deionized water and air dried before examining them by XRF (X-ray fluorescence) based on ASTM standards. The strength of basalt fibers decreased by 58.5 % and the modulus decreased by 31.5 % after 720 h of immersion time. The glass fibers strength reduced by 37 % as compared to the strength measured in the virgin state, and the modulus reduced by 32 %. The comparison showed that the strain and the fracture mechanism of both fiber types were approximately the same but the basalt fiber strength was higher than the strength of the tested glass fibers. For the glass fibers,

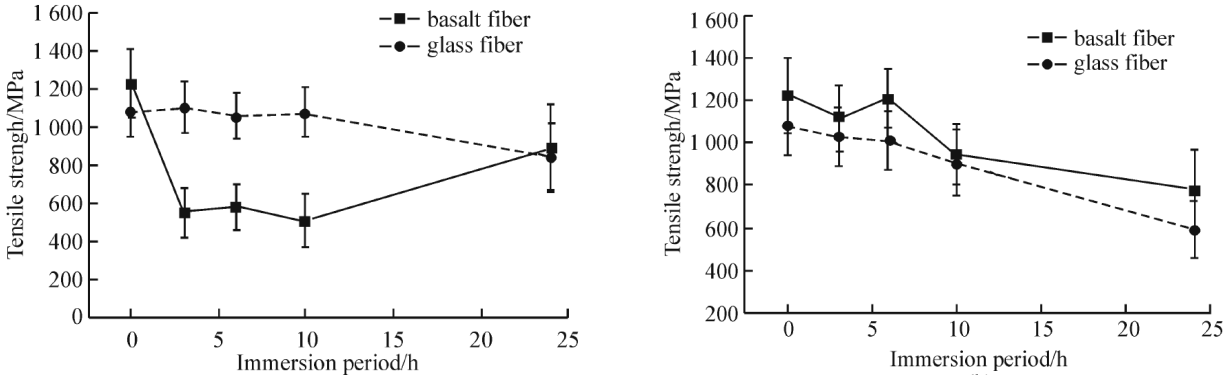

(a) 1mol/L NaOH (b) 2mol/L NaOH

Figure 1.6: Tensile strength of fibers exposed to NaOH solution for 24 h at 100 °C

high content of the Fe^{3+} ions were noted around the generated micro-cracks, while Fe^{3+} ions were seen between separated basalt fibers. The Al^{3+} and Ca^{2+} ions were leached out on the surface of both fiber types throughout immersion, resulting in formation of thick Si layer on the surface.

Wei et al. (2010) studied the tensile behavior of basalt and glass fibers after treating them with 2M HCl (hydrochloric acid) and NaOH (sodium hydroxide) solutions for 0.5 h-3 h. The fibers were first washed in acetone, before treating them with the test solutions and then dried at 105 °C (221 °F) for 3 h. After the treatment, the fibers were soaked in distilled water for 24 h and then dried again. The tensile strengths of fiber bundles were measured before and after treatment. Results showed that the fibers were damaged in both the solutions. Tensile strength of the fibers was inversely proportional to the immersion time, while the effect of acidic solution on basalt fibers was not as high as it was for glass fibers with increased immersion time. The durability of basalt fibers was better in acidic environment than it was in alkaline environment while the durability of glass fibers was identical for both test solutions (Wei et al., 2010).

In a research completed by Mingchao et al. (2008), chemical durability and mechanical properties of alkali-proof basalt fibers and epoxy resin matrix were analyzed. In addition, the mechanical properties of BFRP were studied. First the densities of basalt fibers were measured by using the suspension method (Mingchao et al., 2008). The specimen were then impregnated with resin, and then the tensile properties of the samples were analyzed. The seven day water absorption of the fibers was measured at room temperature. The chemical durability of fiber yarns were tested by boiling them in distilled water, 2 mol/L NaOH and 2 mol/L HCl for 3 h. The mass loss of the fibers was measured and the tensile properties were determined. The BFRP flexural specimen were stored in eight different chemical media (30 % vitriol, 5 % hydrochloric acid, 5 % nitric acid, 110 % sodium hydroxide, saturated sodium carbonate solution, 10 % ammonia, acetone and distilled water) for 15 d, 30 d, and 90 d at room temperature. The results showed that the chemical durability of fibers after 3 h period in hydrochloric acid was much less in comparison to sodium hydroxide. The mass of fibers, and their tensile strength decreased more after exposing them to hydrochloric acid in comparison to exposure in sodium hydroxide. The flexural strength of the BFRP specimen kept lowering while the flexural modulus was steady in alkaline media, but both the flexural strength and modulus decreased after exposure in acid media(Mingchao et al., 2008).

1.6 Sizing

The sizing is a protective layer that is applied to the virgin fibers at the end of the manufacturing process. Sizing forms a strong protective layer, which shields each fiber from chemical attacks in aggressive environments and mechanical damage, but it also increases the resin adhesion to the fiber (Ivashchenko, 2009). A number of studies were conducted to improve the alkali resistance throughout the application of different sizing agents and to match it properly to the fibers (Rybin et al., 2016). Some of the methods researchers developed are: modifying the makeup of fibers by addition of alkali resistant components such as ZrO_2 to the raw materials (Lipatov et al., 2015), applying alkali resistant coating to the fibers (Jung and Subramanian, 1994; Rybin et al., 2013), and modifying cement matrices by using special additives (Lipatov et al., 2012).

1.7 Chemical Durability Studies on Sizing

Rybin et al. (2013), conducted a study to compare the tensile strength characteristics of virgin basalt fibers to Zirconia-coated basalt fibers. The fibers were coated with Zirconyl Chloride Octahydrate ($ZrCl_2 \cdot 8\,H_2O$ [0.1–0.4M]) and heated in a furnace at 550 °C (1022 °F) for half an hour in argon atmosphere and then cooled in air. The fibers were then exposed to alkali solution for a duration of eight days. According to this study the Zircona coting helped improve the corrosion resistance of the fibers. The tensile strength of virgin fibers and 0.4M zirconia-coated fibers immersed in alkali for eight days was 4.5 GPa and 4.4 GPa, respectively which is a 0.1 GPa difference. But the 0.1M zirconia coated fibers reached only 2.6 GPa after eight-day exposure (Rybin et al., 2013). Further, the uncoated and coated fibers were tested in a cement matrix, and zirconia coating made the fibers more resistant to corrosion from the alkali environment.

Rybin et al. (2016) coated basalt fibers with zirconium dioxide and titanium dioxide, and studied the corrosion behavior after exposing the coated fibers to 2M NaOH (sodium hydroxide, pH14) and saturated 0.02M Ca(OH) 2 (calcium hydroxide) for 16 d and 64 d. Zirconyl-chloride octahydrate ($ZrOCl_2 \cdot 8\,H_2O$) was dissolved in ethanol water to form a 0.4M ZrO_2 solution, which was aged for three days before it was used to coat the fibers. Titanium tetrachloride ($TiCl_4$) was added to frozen water to form 0.8M TiO_2 solution. The basalt fibers were immersed into the solutions for 1 min and then air dried before aging them in a preheated furnace at 550 °C, which prevented degradation of mechanical properties of fiber. The specimens were cleaned twice with distilled water after the exposure period and dried at room temperature. The cleaned dry specimens were scanned using scanning electron microscope (SEM), and energy-dispersive X-ray method (EDS). Rybin et al. (2016) found that the degradation of coated fibers was less than the degradation of non-coated fibers. TiO_2 coating helped protecting fibers from early degradation in $CaOH_2$ solution, and ZrO_2 coating protected fibers in both solutions.

In research projects performed by Wei (Wei et al. (2011) and Wei et al. (2011)), the surface of basalt fibers were modified by organic/inorganic nano hybrid sizing synthesized using sol-gel technology. The infrared (IR) and atomic force microscopy (AFM) analyses were performed to confirm that the epoxy/SiO_2 nano-hybrid material synthesis was successful. Wei et al. (2011) analyzed the surface morphology of modified fibers and studied the multifilament yarn tensile strength as well as the inter-layer shear strength (ILSS). The predominant method of synthesizing nano SiO_2 is called stöber method (Van Blaaderen et al., 1992). E-51 epoxy resin and 3-Aminopropyltriethoxysilane (KH-550) — at the material ratio of 100:3.55 — were mixed to prepare a modified epoxy resin and stirring at 50 °C-55 °C for 4 h (Wei et al., 2011). Nano-hybrid composite was prepared by mixing nano-SiO_2 solutions with modified epoxy solutions. The ultimate slurry that was used to modify the basalt fiber was made by mixing the epoxy/SiO_2 nano-hybrid material and acetone at a mass ratio of 2:100 (Wei et al., 2011). The results showed that the tensile strength of basalt fiber multifilament yarn was increased by 15 %-30 % after modification (Wei et al. (2011) and Wei et al. (2011)). Surface modification performed well when the SiO_2 content was set to 5 %. A 10 % to 15 % increase in the ILSS of basalt fiber composite was noted (Wei et al. (2011) and Wei et al. (2011)).

1.8 Binder Materials and Types

Resin is the binding material used in the manufacture of FRP to guarantee a unified behavior of the combined fibers. Resin helps to hold the sized fibers together and plays an important role in the load transfer. The resin also protects the fiber from chemical attacks and protects the filaments from mechanical damages (Benmokrane et al., 2002). Resins are classified into two types, Thermosetting resins and Thermoplastic resins. The thermosetting resins are used to manufacture FRP materials for civil structures because after they are cured at high temperatures and hardened, they cannot be returned into a liquid state (Bagherpour, 2012). Thermoplastic resins are not used in civil structures because, they can be returned to their original state by applying heat (reheating). The most common resins used in FRP manufacturing are Epoxy resin, Polyester resin, and Vinyl-Ester resin (ACI Committee 440, 2007). Figure 1.7 shows thermoset resin in its virgin state. The thermoset resins are usually liquid at room temperature and solid with a low melting point in their virgin state. Heat treatment and catalysts are used in the curing process to expedite hardening and set. Table 1.8 shows the properties of typical resin matrices according to Nanni et al. (2014). The following subsections below provide a brief description of the three common resins used in FRP manufacture.

Figure 1.7: Thermoset resin used in FRP

Table 1.8: Typical properties of resins (Nanni et al., 2014)

Type of resin	Density (lb/yd^2)	Tensile Strength (ksi)	Longitudinal Modulus (ksi)	Poissons's ratio	CTE 10^{-6}/°F	Moisture Content (%)	Glass transition Temperature °F
Epoxy	2000−2400	5−15	300−500	0.35−0.39	1.6−3.0	0.15−0.60	203−347
Polyester	2000−2400	7−19	400−600	0.38−0.40	1.3−1.9	0.08−0.15	158−212
Vinyl ester	1900−2300	10−11	435−500	0.36−0.39	1.5−2.2	0.14−0.30	158−329

$Notes: 1lb/yd^3 = 0.593kg/m^3; 1ksi = 6.89N/mm^2; °\text{F} = (9/5 * °\text{C} + 32)$

1.8.1 Epoxy

Epoxy resins are used in high performance composite materials because of the desired mechanical properties of these resins. Epoxies are generally durable and resist chemical attacks and corrosive liquids. The shrinkage characteristic of epoxy is very low, which facilitates its use in civil structures. Epoxy resins are highly viscous and need post curing at elevated temperatures (ACI Committee 440, 2007). Carbas et al. (2013) analyzed the effects of post curing on the mechanical properties (yield strength, Young's modulus, and failure strain) of these resins. The glass transition temperature (T_g) was measured by a dynamic mechanical analysis apparatus developed by Carbas et al. (2013). If epoxy resins are exposed to elevated temperature less than that of glass transition temperature for longer periods, the mass density of the resins increases, which is termed physical aging (Carbas et al., 2013). For the use of resins in civil engineering purposes, the degradation due to decrease in the T_g is not critical if the glassy state is maintained (Arias et al., 2018). Epoxy resins are manufactured by using bisphenol A (BPA), a compound that can be synthesized as a chemical oestrogen (Dodds and Lawson, 1936). BPA leads to a negative impact on the environment, and therefore, researchers started studying the materials that can substitute BPA and allowing the synthesis of epoxy thermoset resins without BPA (Aouf et al., 2013). These types of resins are called bio-epoxies, and are favored by the manufacturers in the production of FRP rebars which make them eco-friendly rebars. The cost of these resins is high compared to other resins and these are widely used in FRP for concrete repair because of high strength

performances (Bagherpour, 2012).

1.8.2 Vinyl-Ester

Vinyl esters are corrosion resistant themoset resins with good mechanical properties (Nouranian et al., 2013; McConnell, 2010; ACI Committee 440, 2007). They are polymeric resins that can be cured faster than epoxy resins, and can be cured in both room temperature and at elevated temperatures (Cook et al., 1997). The flexural properties of a neat vinyl ester resin depends on the curing atmosphere (Nouranian et al., 2013). Figure 1.8 shows the chemical structure of a vinyl ester prepolymer. These resins are used in civil engineering

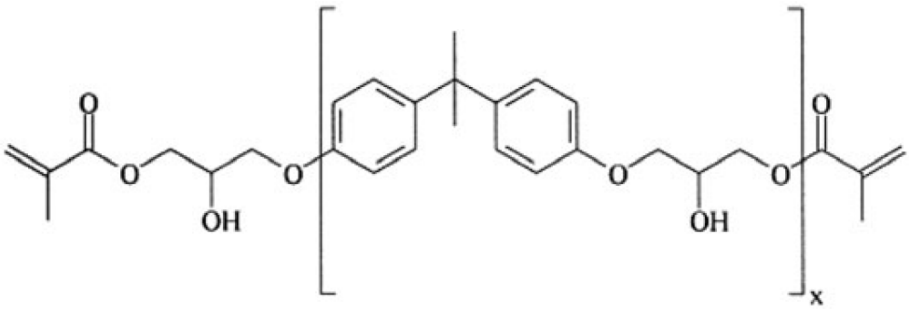

Figure 1.8: Structure of a vinyl-ester

structures not only because of their good mechanical properties but also because of their good toughness and low shrinkage properties when cured (Alia et al., 2013). The mechanical properties of these resins, and their viscoelastic properties are affected by post-curing temperature (Alía et al., 2015). These resins are cheaper and have better physical and mechanical properties in comparison to other resins. The glass fiber industry uses vinyl-ester resin predominantly while epoxy resins are used in basalt fiber industry (Nanni et al., 2014).

1.8.3 Polyester

Polyesters are unsaturated reins with good mechanical performance, low material density, and high chemical resistance (Fink, 2017). One of the main reasons to use these low cost resins in the civil engineering industry is, they are adaptable into large composite structures (Baley et al., 2006). The curing process involves dissolving resin in the monomer, which reacts with unsaturated polymer to form thermoset structure (ACI Committee 440, 2007). These resins shrink about 7 % during the curing process leading to problems such as surface distortion, or inability to mold to close parts, etc. (Kinkelaar et al., 1994). Low profile additives like thermoplastic polymers are added to overcome such problems with curing (Huang and Liang, 1996). However, different types of resins exist to satisfy different desirable requirements such as dimensional stability, cost efficiency, etc.

1.9 Chemical Durability Studies on Resins

In a study completed by Benmokrane et al. (2017), the durability of glass fiber rebars made with vinyl-ester, isophthalic polyester, and epoxy resins after alkaline exposure for 1000, 3000 and 5000 h at elevated temperatures (60 °C [140 °F]) was evaluated. GFRP rebars with a 12 mm diameter were tested for this study because small sized specimen suffer more severely from chemical attacks. The physical and mechanical properties of the rebar were measured according to ASTM standards before and after the immersion period. Then, they were compared to one another. The comparison between rebars made with three different types of resin showed that the rebar made from polyester resin had the lowest virgin and conditioned physical and mechanical properties. The epoxy and vinyl-ester GFRP bars had higher fiber-resin bond, flexural strength, flexural modulus of elasticity, and inter-laminar-shear strength while having the least moisture uptake. The flexural strength reduction of polyester, vinyl-ester, and epoxy resin were 25 %, 17 %, and 23 %, respectively.

The inter-laminar shear strength of rebars made with polyester resin was reduced by 21 % while the strength of rebars made from vinyl-ester, and epoxy resin was reduced by only 13 %. Finally, the polyester GFRP absorbed 18 % more water in comparison to other rebars.

In a research conducted by Kajorncheappunngam et al. (2002), glass reinforced epoxy coupons were immersed in four different liquid media at two different temperatures, and the durability of coupons was evaluated. Epoxy compatible E-glass fibers were woven with epoxy resin and soaked in distilled water, saturated salt solution (30 g/ 100 cc NaCl), 5M NaOH solution, and a 1M hydrochloric acid (HCl) solution for 5 months, and aged at room temperature and at 60 °C (140 °F). The tensile and durability properties of the coupons were analyzed, and SEM analysis of aged coupons was performed. The results of tensile strength tests on the epoxy neat resin and the fiber-resin coupons are listed in Tables 1.9, 1.10, 1.11, and 1.12. Tables 1.9 and 1.10 show the tensile strength results of the epoxy resin exposed to liquid media in room temperature and at elevated temperature. The tensile test results of the fiber-resin coupons can be found in Tables 1.11, and 1.12. It can be seen that the strength retention of GFRP rebars made from epoxy resin in alkali environment was high at both room temperature and elevated temperature. Results of this study demonstrated that the epoxy resins are durable in alkali environment and the durability of GFRP coupons depends on the resistance of glass fiber to aggressive environments.

Table 1.9: Effect of liquid media at room temperature on the tensile properties of epoxy neat resin (Kajorncheappunngam et al., 2002)

		Solutions												
		Saturated Salt (NaCl)			5M NaOH			Distilled Water			1M HCl			Control Sample
		Aging Time (month)			Aging Time (month)			Aging Time (month)			Aging Time (month)			Aging Time(month)
Properties	Unit.	1	3	5	1	3	5	1	3	5	1	3	5	0
Maximum Stress at Failure	psi	6707	5336	5057	8572	7229	5821	5915	6706	5677	6159	4551	4564	5558
Strain at Failure	microstrain	22329	11899	10585	28823	24619	13647	13261	20649	15426	10024	9335	9516	11730
Young's Modulus	msi	0.45	0.48	0.52	0.44	0.41	0.47	0.53	0.44	0.42	0.66	0.52	0.51	0.51
Percent Maximum Stress Reduction [a]	%	-20.68(120.68)	4.00(96.00)	9.00(91.00)	-54.22(154.22)	-30.07(130.07)	-4.74(104.74)	-6.43(106.43)	-20.66(120.66)	-2.14(102.14)	-10.81(110.81)	18.12(81.88)	17.88(82.12)	–
Percent Ultimate Strain Reduction	%	-90.89	-1.44	9.76	-145.71	-109.87	-16.34	-13.05	-76.03	-31.51	14.54	20.41	18.87	–

Table 1.10: Effect of liquid media at elevated temperature on the tensile properties of epoxy neat resin (Kajorncheappunngam et al., 2002)

		Solutions												
		Saturated Salt (NaCl)			5M NaOH			Distilled Water			1M HCl			Control Sample
		Aging Time (month)			Aging Time (month)			Aging Time (month)			Aging Time (month)			Aging Time(month)
Properties	Unit.	1	3	5	1	3	5	1	3	5	1	3	5	0
Maximum Stress at Failure	psi	5554	5013	4783	6719	5001	4713	5801	5312	5332	4492	5335	5670	5558
Strain at Failure	microstrain	14458	12543	11518	18251	12519	11132	15600	14379	13413	10107	10424	12929	11730
Young's Modulus	msi	0.44	0.45	0.47	0.42	0.43	0.47	0.43	0.43	0.45	0.49	0.52	0.49	0.51
Percent Maximum Stress Reduction [b]	%	0.08(99.92)	9.81(90.19)	13.94(86.06)	-20.88(120.88)	10.02(89.98)	15.20(84.80)	-4.37(104.37)	4.43(95.57)	4.06(95.94)	19.17(80.83)	104244.01(95.99)	-2.01(102.01)	–
Percent Ultimate Strain Reduction	%	-23.25	-6.94	1.81	-55.59	-6.73	5.09	-32.99	-22.58	-14.34	13.83	11.13	-10.22	–

[a]Parentheses indicate the percentage retention of tensile strength.
[b]Parentheses indicate the percentage retention of tensile strength.

Table 1.11: Effect of liquid media at room temperature on the tensile properties of glass/epoxy composite (Kajorncheappunngam et al., 2002)

		Solutions												
		Saturated Salt (NaCl)			5M NaOH			Distilled Water			1M HCl			Control Sample
		Aging Time (month)			Aging Time (month)			Aging Time (month)			Aging Time (month)			Aging Time(month)
Properties	Unit.	1	3	5	1	3	5	1	3	5	1	3	5	0
Maximum Stress at Failure	psi	54368	56640	59688	43900	46851	41825	58413	47333	44458	29007	17711	15324	57920
Strain at Failure	microstrain	19452	20092	20649	17125	16352	14916	19226	16025	15288	11005	7431	6284	20664
Young's Modulus	msi	2.90	3.00	3.00	3.04	3.23	3.04	3.17	3.05	2.97	2.83	2.49	2.52	3.05
Percent Maximum Stress Reduction [a]	%	6.1(93.87)	2.21(97.79)	-3.05(103.50)	24.12(75.79)	19.11(80.89)	27.79(72.21)	-0.85(100.85)	18.28(81.72)	23.24(76.76)	49.94(50.08)	69.42(30.58)	73.54(26.46)	–
Percent Ultimate Strain Reduction	%	5.87	2.77	0.07	17.13	20.86	27.81	6.96	22.45	26.02	46.74	64.04	69.59	–

Table 1.12: Effect of liquid media at elevated temperature on the tensile properties of glass/epoxy composite (Kajorncheappunngam et al., 2002)

		Solutions												
		Saturated Salt (NaCl)			5M NaOH			Distilled Water			1M HCl			Control Sample
		Aging Time (month)			Aging Time (month)			Aging Time (month)			Aging Time (month)			Aging Time(month)
Properties	Unit.	1	3	5	1	3	5	1	3	5	1	3	5	0
Maximum Stress at Failure	psi	54196	57721	46735	27172	15591	15363	29405	30503	30262	37350	37771	30087	57920
Strain at Failure	microstrain	20158	20429	17314	11425	7099	6191	10205	10043	10122	16223	12846	13437	20664
Young's Modulus	msi	2.82	3.15	2.80	2.79	2.76	2.79	2.94	3.09	3.07	2.55	2.33	2.46	3.05
Percent Maximum Stress Reduction [b]	%	6.43(93.57)	0.34(99.66)	19.31(80.69)	53.03(46.91)	73.08(26.92)	73.47(26.53)	49.23(50.77)	47.34(52.66)	47.75(52.25)	35.51(64.49)	34.79(65.21)	48.05(51.95)	–
Percent Ultimate Strain Reduction	%	2.32	1.13	16.21	44.71	65.64	70.04	50.61	51.39	51.02	21.49	37.83	34.97	–

[a]Parentheses indicate the percentage retention of tensile strength.
[b]Parentheses indicate the percentage retention of tensile strength.

1.10 BFRP Rebar Production

By analyzing the SEM pictures of the surface of FRP rebars, manufactures believe that numerous properties are influenced by the production process (Borges et al., 2015). Based on this, FRP rebar manufacturers developed several processes to help increase the efficiency and quality of production. Because the production process for FRP rebars is not standardized yet, many different BFRP rebar products are available in the market with dissimilar physical and mechanical properties (Borges et al., 2015; Joshi et al., 2003). The most predominant methods are pultrusion, wet-layup, and braiding or weaving. In the BFRP rebar industry, the most common manufacturing methods are pultrusion and wet-layup, while the manufacturers seem to prefer pultrusion process due to the efficiency and economical factors. Braiding is an old production process for FRPs and manufacturers seem to not use this process due to the inconsistency in surface properties of the rebar. Because pultrusion and wet-layup processes are the most common techniques for the production of FRP materials, they are described in the following subsections.

1.10.1 Wet-Layup

The wet-layup process was invented because of the increasing demand for the FRP rebars in the infrastructure rehabilitation (Saadatmanesh et al., 2010). Manufacturers believe that this process is economical in comparison to the traditional pultrusion process. It is a recently developed process and has not been widely researched, yet. Figure 1.9 schematically represents the wet-layup process to show how the fibers are guided through a resin bath in which the wetting of fibers in resin and impregnation occurs. A programmable arm

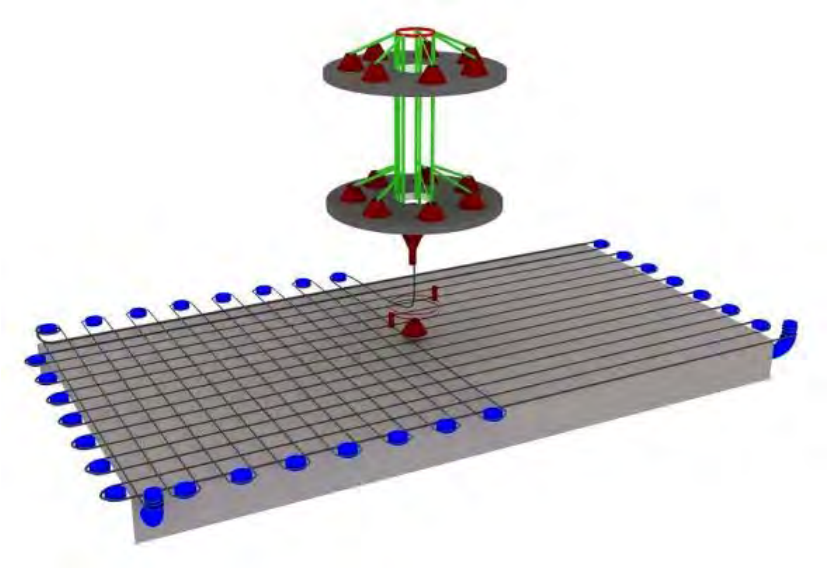

Figure 1.9: Schematic of wet-layup process (Banibayat, 2011)

with three degrees of freedom in orthogonal direction helps in rebar manufacturing. Though this process is economical, manufacturers do not prefer this method because of potential inconsistencies in rebar dimensions and surface properties. The rebar manufactures who use this process generally produce rebars with wavy surface, which helps to improve the bond-to-concrete strength but reduces the tensile strength of the rebar (You et al., 2015).

1.10.2 Pultrusion

Pultrusion is the most predominant method that manufacturers use to produce FRP rebars. It is a fully automated process, and hence the most economical and time-saving method. The fibers and the resin are molded in a continuous process that helps maintain a consistent rebar cross section. Figure 1.10 schematically represents the pultrusion process (Borges et al., 2015), in which the fibers are first cleaned and parallelized in the rovings before entering the resin bath. In the resin bath, the fibers are impregnated with resin at

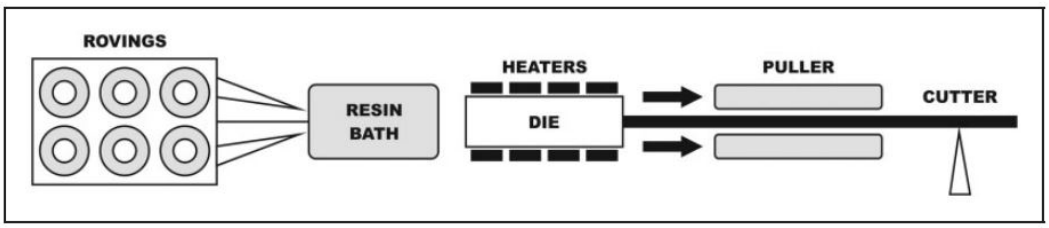

Figure 1.10: Schematic representation of the pultrusion process (Borges et al., 2015)

suitable temperatures between 30 °C to 50 °C (86 °F to 122 °F) range (Borges et al., 2015). The viscosity of the resin increases as the temperature increases, possibly resulting in improper impregnation. The wet fibers then enter into the heating die with multiple heating zones which activates the curing process, to ensure that the resin hardens and bonds the fibers together, producing a uniform FRP rebar. In a research conducted by Joshi et al. (2003), the authors claimed that the recommended curing temperature is 177 °C (350 °F). An exothermic reaction helps the liquid resin to form into a gel, which later harden into a fiber-resin matrix. The fiber-resin composite is then pulled out of the machine and cooled to room temperature. Following this process, a surface enhancement (sand coating, ribs, and surface lugs) is applied to the outer part of the rebars, which increases the bond-to-concrete strength (You et al., 2015). Quality of the rebar is affected by the resin quality, production time, curing temperature, fiber content and other factors.

1.11 Chemical Durability Studies on FRP Rebar

In a study performed by Guo et al. (2018), the durability of CFRP, GFRP, and BFRP immersed in various chemically active solutions at 60 °C (140 °F) was analyzed. The solutions used and their chemical composition are listed in Table 1.13. The results obtained from samples immersed in the distilled water were used as a reference. The alkaline content of SWSS concrete solutions was low in comparison to normal concrete

Table 1.13: Chemical composition of accelerated solutions (Guo et al., 2018)

	Quantities(g/Ll)				
Simulated Environment	NaOH	KOH	$Ca(OH_2)$	NaCl	pH
SWSSNC[1]	2.4	19.6	2.0	35	13.4
NC[2]	2.4	19.6	2.0	–	13.4
SWSSHPC[3]	0.6	1.4	0.037	35	12.7
HPC[4]	0.6	1.4	0.037	–	12.7
DW[5]	–	–	–	–	7.5

because of added slag that replaced Portland cement. FRP coupons were stored in sealed containers to prevent calcium hydroxide from interacting with carbon dioxide in the air. The specimen were immersed in solutions for 90 d, and the moisture uptake of all the rebars in the various solutions was as follows: NC > SWSSNC > DW > HPC > SWSSHPC. The FRP in HPC and SWSSHPC followed a distinct trend, which indicated that the alkali content play an important role in the durability of FRP. The moisture uptake of FRP in SWSSHPC and SWSSNC was lower than that of NC and HPC , which indicated that the seawater and sea sand played a beneficial role in resisting water uptake or degradation. However, the water uptake of BFRP rebars in NC was lower than SWSSNC at the end of 90 d, which showed that NaCl present in SWSSNC

plays a key role in preventing the deterioration of BFRP. CFRP had the better durability in comparison to other FRP.

Benmokrane et al. (2015) performed an experimental analysis of physical, mechanical, and durability properties of BFRP rebar manufactured with vinyl ester resin, GFRP-vinyl ester resin, and BFRP-epoxy resin. The physical and mechanical properties of the unconditioned rebars were first measured. These results were used as the reference results to compare the properties of the rebars after exposure to alkaline environments that simulated the concrete pore solution at 60 °C (140 °F) for 1000 h, 3000 h, and 5000 h. Differential scanning calorimetry (DSC) was used to measure the glass transition temperature and Fourier transform infrared spectroscopy (FTIR) was used to measure the chemical composition of the rebars. Scanning electron microscope (SEM) was used to evaluate the micro structure of the un-aged and the aged samples. The results showed that the moisture absorption of both types of unconditioned basalt rebars was almost twice as much as the GFRP rebar. GFRP rebars also had a higher inter-laminar shear strength, flexural strength, flexural modulus of elasticity, and had a good fiber-resin bond in comparison to BFRP rebars. BFRP-Vinyl ester, unconditioned rebars had the lowest transverse shear strength, flexural strength, inter-laminar shear strength, and weak fiber/resin interface (Benmokrane et al., 2015). The transverse strength of conditioned BFRP-vinyl ester bars reduced by 33 %, while GFRP-vinyl ester and BFRP-epoxy bars decreased by 9 % and 10 % , respectively. In addition, the flexural strength of both the BFRP rebars decreased by 37 % and GFRP rebars by 7 %. Interlaminar shear strength of BFRP-vinyl ester bars decreased by 22 %, BFRP-epoxy reabrs decreased by 14 % and GFRP rebars decreased by 5 %. Ultimately, the GFRP rebar showed the better durability in alkaline environment in comparison to BFRP rebars.

Chapter 2

Existing Standards for FRP rebars

In this chapter, the existing standards and acceptance criteria for GFRP and BFRP rebars in concrete structures according to various national and international regulations are presented in table format. Table 2.1 lists the various codes and standards for countries/nations that provide acceptance criteria for FRP rebars with various sizes.

Table 2.1: Codes and standards for FRP in different countries

Code	Country	Year
FDOT 932-3	USA (Florida)	2017
AC454	USA	2017
ASTM D 7957	USA	2017
CAN/CSA S807	Canada	2010 (R2015)
FIB Bulletin 40	Europe	2007
GOST 31938	Russia	2012

2.1 Typical Fiber Properties

Typical properties of basalt, E-glass, and S-glass fibers according to FIB Bulletin 40 are listed in Table 2.2, and 2.3 in imperial and metric units (rounded to the nearest two decimal values).

Table 2.2: Acceptance criteria for properties of fibers for the production of FRP rebars (Imperial Units)

		Fiber Type (FIB Bulletin 40)		
		Basalt	Glass	
Properties	units.		E- glass	S- glass
Density	lbs./ft^3	174.8	156.07	156.07
Tensile Strength	ksi	701.98	500.38	664.26
Young's Modulus	ksi	12 908.4	10 500.73	12 400.73
Ultimate Tensile Strain	%	3.1	2.5	3.3
Coefficient of Thermal Expansion	10^{-6}/°C	8	5	2.9
Poisson's Coefficient	–	–	0.22	0.22

Table 2.3: Acceptance criteria for properties of fibers for the production of FRP rebars (Metric Units)

		Fiber Type (European)		
		Basalt	Glass	
Properties	units.		E- glass	S- glass
Density	kg/m^3	2800	2500	2500
Tensile Strength	MPa	4840	3450	4580
Young's Modulus	GPa	89	72.4	85.5
Ultimate Tensile Strain	%	3.1	2.5	3.3
Coefficient of Thermal Expansion	10^{-6}/°C	8	5	2.9
Poisson's Coefficient	–	–	0.22	0.22

2.2 Typical Resin Properties

Typical properties of polyester, epoxy, and vinyl ester resins according to FIB Bulletin 40 are listed in the Tables 2.4 and 2.5 in imperial and metric units (rounded to the nearest two decimal values), respectively.

Table 2.4: Acceptance criteria for properties of resins for the production of FRP rebars (Imperial Units)

		Resin Type (FIB Bulletin 40)		
Properties	units.	Polyester	Epoxy	Vinyl ester
Density	lbs./ft^3	74.91 – 87.4	74.91 – 87.4	71.79 – 84.28
Tensile Strength	ksi	5.00 – 15.08	7.98 – 18.85	10.59 – 11.75
Longitudinal Modulus	ksi	304.58 – 513.43	398.85 – 594.66	435.11 – 507.63
Poisson's Coefficient	–	0.35 – 0.39	0.38 – 4.0	0.36 – 0.39
Coefficient of Thermal Expansion	10^{-6}/°C	55 – 100	45 – 65	50 – 75
Moisture Content	%	0.15 – 0.60	0.08 – 0.15	0.14 – 0.30

Table 2.5: Acceptance criteria for properties of resins for the production of FRP rebars (Metric Units)

		Resin Type (European)		
Properties	units.	Polyester	Epoxy	Vinyl ester
Density	kg/m^3	1200 – 1400	1200 – 1400	1150 – 1350
Tensile Strength	MPa	34.50 – 104	55 – 130	73 – 81
Longitudinal Modulus	GPa	2.10 – 3.45	2.75 – 4.10	3.00 – 3.50
Poisson's Coefficient	–	0.35 – 0.39	0.38 – 4.0	0.36 – 0.39
Coefficient of Thermal Expansion	10^{-6}/°C	55 – 100	45 – 65	50 – 75
Moisture Content	%	0.15 – 0.60	0.08 – 0.15	0.14 – 0.30

2.3 Cross Sectional Properties of Rebar

Tables 2.6, and 2.7 show the required cross section diameter and the cross-sectional areas for the rebars of different sizes in imperial units. Tables 2.8, and 2.9 list the same data in metric units (rounded to the nearest two decimal values). The first column of the tables represents the rebar number. While standards in Europe, Canada and Russia follow a different numbering system for rebars, the converted dimensions are given in the table for ease of comparison.

Table 2.6: Acceptance criteria for cross section measurements of GFRP rebar (Imperial Units)

	GFRP											
	FDOT 932-3/2017		AC454		ASTM D 7957		CAN/CSA S807		FIB Bulletin 40		GOST 31938 -2012	
	Diameter	Area	Diameter	Area	Diameter	Area	Diameter	Area	Diameter	Area	Diameter	Area
Bar Size	in.	$in.^2$	in.	$in.^2$	in.	$in.^2$	in.	$in.^2$	in.	$in.^2$	in.	$in.^2$
1	n/a	n/a	n/a	n/a	n/a	n/a	0.24	0.05	0.24	0.04	0.24	n/a
2	0.25	0.046 - 0.085	0.25	0.046 - 0.085	0.25	0.046 - 0.085	0.31	50.08	0.31	0.08	0.31	n/a
3	0.370	0.104 - 0.161	0.370	0.104 - 0.161	0.370	0.104 - 0.161	0.39	0.11	0.39	0.12	0.39	n/a
4	0.500	0.185 - 0.263	0.500	0.185 - 0.263	0.500	0.185 - 0.263	0.51	0.2	0.47	0.18	0.47	n/a
5	0.625	0.288 - 0.388	0.625	0.288 - 0.388	0.625	0.288 - 0.388	0.59	0.31	0.55	0.24	0.55	n/a
6	0.750	0.415 - 0.539	0.750	0.415 - 0.539	0.750	0.415 - 0.539	0.79	0.44	1.00	0.31	1.00	n/a
7	0.875	0.565 - 0.713	0.875	0.565 - 0.713	0.875	0.565 - 0.713	0.87	0.6	0.79	0.49	0.7	n/a
8	1.000	0.738 - 0.913	1.000	0.738 - 0.913	1.000	0.738 - 0.913	0.98	0.79	0.98	0.65	0.79	n/a
9	1.128	0.934 - 1.137	1.128	0.934 - 1.137	1.128	0.934 - 1.137	1.18	1.0	1.1	0.95	0.98	n/a
10	1.270	1.154 - 1.385	1.270	1.154 - 1.385	1.270	1.154 - 1.385	1.26	1.27	1.26	1.25	1.1	n/a
11	n/a	n/a	n/a	n/a	n/a	n/a	1.42	1.56	1.56	1.95	1.26	n/a

Table 2.7: Acceptance criteria for cross section measurements of BFRP rebar (Imperial Units)

	BFRP											
	FDOT 932-3/2017		AC454		ASTM D 7957		CAN/CSA S807		FIB Bulletin 40		GOST 31938 -2012	
	Diameter	Area	Diameter	Area	Diameter	Area	Diameter	Area	Diameter	Area	Diameter	Area
Bar Size	in.	$in.^2$	in.	$in.^2$	in.	$in.^2$	in.	$in.^2$	in.	$in.^2$	in.	$in.^2$
1	n/a	n/a	n/a	n/a	n/a	n/a	0.24	0.05	0.24	0.04	0.24	n/a
2	n/a	n/a	n/a	n/a	n/a	n/a	0.31	0.08	0.31	0.08	0.31	n/a
3	n/a	n/a	n/a	n/a	n/a	n/a	0.39	0.11	0.39	0.12	0.39	n/a
4	n/a	n/a	n/a	n/a	n/a	n/a	0.51	0.2	0.47	0.18	0.47	n/a
5	n/a	n/a	n/a	n/a	n/a	n/a	0.59	0.31	0.55	0.24	0.55	n/a
6	n/a	n/a	n/a	n/a	n/a	n/a	0.79	0.44	1.00	0.31	1.00	n/a
7	n/a	n/a	n/a	n/a	n/a	n/a	0.87	0.6	0.79	0.49	0.7	n/a
8	n/a	n/a	n/a	n/a	n/a	n/a	0.98	0.79	0.98	0.65	0.79	n/a
9	n/a	n/a	n/a	n/a	n/a	n/a	1.18	1.0	1.1	0.95	0.98	n/a
10	n/a	n/a	n/a	n/a	n/a	n/a	1.26	1.27	1.26	1.25	1.1	n/a
11	n/a	n/a	n/a	n/a	n/a	n/a	1.42	1.56	1.56	1.95	1.26	n/a

Table 2.8: Acceptance criteria for cross section measurements of GFRP rebar (Metric Units)

	GFRP											
	FDOT 932-3/2017		AC454		ASTM D 7957		CAN/CSA S807		European		GOST 31938 -2012	
	Diameter	Area	Diameter	Area	Diameter	Area	Diameter	Area	Diameter	Area	Diameter	Area
Bar Size	in.	in.^{2}	in.	in.^{2}	in.	in.^{2}	mm	mm^2	mm	mm^2	mm	mm^2
1	n/a	n/a	n/a	n/a	n/a	n/a	6	32	6	28.3	6	n/a
2	6.35	29.68 - 54.84	0.025	0.046 - 0.085	0.025	0.046 - 0.085	8	50	8	50.3	8	n/a
3	9.4	67.1 - 103.87	0.370	0.104 - 0.161	0.370	0.104 - 0.161	10	71	10	78.5	10	n/a
4	12.7	119.35 - 152.26	0.500	0.185 - 0.263	0.500	0.185 - 0.263	13	129	12	113	12	n/a
5	15.88	185.81 - 250.32	0.625	0.288 - 0.388	0.625	0.288 - 0.388	15	199	14	154	14	n/a
6	19.05	267.74 - 347.74	0.750	0.415 - 0.539	0.750	0.415 - 0.539	20	284	16	201	16	n/a
7	22.23	364.52 - 463.87	0.875	0.565 - 0.713	0.875	0.565 - 0.713	22	387	20	314	18	n/a
8	25.4	507.74 - 589.03	1.000	0.738 - 0.913	1.000	0.738 - 0.913	25	510	25	419	20	n/a
9	28.65	602.58 - 733.55	1.128	0.934 - 1.137	1.128	0.934 - 1.137	30	645	28	616	25	n/a
10	32.26	744.51 - 893.55	1.270	1.154 - 1.385	1.270	1.154 - 1.385	32	819	32	804	28	n/a
11	n/a	n/a	n/a	n/a	n/a	n/a	36	1006	40	1257	32	n/a

Table 2.9: Acceptance criteria for cross section measurements of BFRP rebar (Metric Units)

	BFRP											
	FDOT 932-3/2017		AC454		ASTM D 7957		CAN/CSA S807		European		GOST 31938 -2012	
	Diameter	Area	Diameter	Area	Diameter	Area	Diameter	Area	Diameter	Area	Diameter	Area
Bar Size	in.	in.^{2}	in.	in.^{2}	in.	in.^{2}	mm	mm^2	mm	mm^2	mm	mm^2
1	n/a	n/a	n/a	n/a	n/a	n/a	6	32	6	28.3	6	n/a
2	n/a	n/a	n/a	n/a	n/a	n/a	8	50	8	50.3	8	n/a
3	n/a	n/a	n/a	n/a	n/a	n/a	10	71	10	78.5	10	n/a
4	n/a	n/a	n/a	n/a	n/a	n/a	13	129	12	113	12	n/a
5	n/a	n/a	n/a	n/a	n/a	n/a	15	199	14	154	14	n/a
6	n/a	n/a	n/a	n/a	n/a	n/a	20	284	16	201	16	n/a
7	n/a	n/a	n/a	n/a	n/a	n/a	22	387	20	314	18	n/a
8	n/a	n/a	n/a	n/a	n/a	n/a	25	510	25	419	20	n/a
9	n/a	n/a	n/a	n/a	n/a	n/a	30	645	28	616	25	n/a
10	n/a	n/a	n/a	n/a	n/a	n/a	32	819	32	804	28	n/a
11	n/a	n/a	n/a	n/a	n/a	n/a	36	1006	40	1257	32	n/a

2.4 Minimum Guaranteed Tensile Strength of Rebar

Tables 2.10, and 2.11, list the required minimum guaranteed tensile strength of the rebars in imperial and metric units (rounded to the nearest two decimal values) respectively . The criteria listed in the Canadian standards change for different grades, but the listed information is given for grade I bars.

Table 2.10: Acceptance criteria for tensile strength (Imperial Units)

	GFRP						BFRP					
	FDOT 932-3/2017	AC454	ASTM D 7957	CAN/CSA S807	GOST 31938 -2012	FIB Bulletin 40	FDOT 932-3/2017	AC454	ASTM D 7957	CAN/CSA S807	GOST 31938 -2012	FIB Bulletin 40
Bar Size	ksi	ksi	ksi	ksi	ksi	ksi	ksi	ksi	ksi	ksi	ksi	ksi
1	n/a		n/a	108.78	⩾ 116.03	65.27–232.06	n/a		n/a	TBD	⩾ 116.03	n/a
2	6.1		6.1	108.78			n/a		n/a	TBD		n/a
3	13.2		13.2	108.78			n/a		n/a	TBD		n/a
4	21.6		21.6	94.27			n/a		n/a	TBD		n/a
5	29.1		29.1	94.27			n/a		n/a	TBD		n/a
6	40.9		40.9	87.02			n/a		n/a	TBD		n/a
7	54.1		54.1	79.77			n/a		n/a	TBD		n/a
8	66.8		66.8	79.77			n/a		n/a	TBD		n/a
9	82.0		82.0	72.52			n/a		n/a	TBD		n/a
10	98.2		98.2	65.27			n/a		n/a	TBD		n/a
11	n/a		n/a	65.27			n/a		n/a	TBD		n/a

Table 2.11: Acceptance criteria for tensile strength (Metric Units)

	GFRP						BFRP					
	FDOT 932-3/2017	AC454	ASTM D 7957	CAN/CSA S807	GOST 31938 -2012	FIB Bulletin 40	FDOT 932-3/2017	AC454	ASTM D 7957	CAN/CSA S807	GOST 31938 -2012	FIB Bulletin 40
Bar Size	MPa	MPa	MPa	MPa	MPa	MPa	MPa	MPa	MPa	MPa	MPa	MPa
1	n/a		n/a	750	⩾ 800	450–1600	n/a		n/a	TBD	⩾ 800	n/a
2	0.88		0.88	750			n/a		n/a	TBD		n/a
3	13.2		13.2	750			n/a		n/a	TBD		n/a
4	21.6		21.6	650			n/a		n/a	TBD		n/a
5	29.1		29.1	650			n/a		n/a	TBD		n/a
6	5.93		5.93	600			n/a		n/a	TBD		n/a
7	7.84		7.84	550			n/a		n/a	TBD		n/a
8	66.8		66.8	550			n/a		n/a	TBD		n/a
9	82.0		82.0	500			n/a		n/a	TBD		n/a
10	14.24		14.24	450			n/a		n/a	TBD		n/a
11	n/a		n/a	450			n/a		n/a	TBD		n/a

2.5 Physical and Mechanical Properties of Rebar

The required physical and mechanical properties of the rebars are tabulated in the Table 2.12, and Table 2.13. The first column of the table lists the test methods used to determine those properties in the U.S. and Canada. The criteria listed in the Canadian standards are given for grade I bars (criteria changes for different grades).

Table 2.12: Acceptance criteria for physical and mechanical characteristics of GFRP rebar (Imperial Units)

			GFRP					
			FDOT 932-3/2017	AC454	ASTM D 7957	CAN/CSA S807	FIB Bulletin 40	GOST 31938 -2012
Test Method	Test Description	Unit	Criteria	Criteria	Criteria	Criteria	Criteria	Criteria
ASTM D 2584	Fiber Content	% wt.	$\geqslant 70$	$\geqslant 70$	$\geqslant 70$	$\geqslant 55$	$\geqslant 0.55$	n/a
ASTM D 570	Moist. Absorption short term @50 °C	%	$\leqslant 0.25$	$\leqslant 0.25$	$\leqslant 0.25$	$\leqslant 0.35$	n/a	n/a
ASTM D 570	Moist. Absorption long term @50 °C	%	$\leqslant 1.0$	n/a	$\leqslant 1.0$	$\leqslant 1.0$	n/a	n/a
ASTM D 7617	Min. Guaranteed Transverse Shear	ksi	$\geqslant 22$	$\geqslant 22$	$\geqslant 19$	$\geqslant 23.21$	$\geqslant 39$	n/a
ASTM D 4475	Horizontal Shear Stress	ksi	n/a	$\geqslant 5.5$	n/a	TBD	$\geqslant 89$	n/a
ACI440. 3 R,B.3	Bond-to-concrete strength	ksi	$\geqslant 1.1$	$\geqslant 1.1$	$\geqslant 1.1$	> 1.16	n/a	$\geqslant 1.74$

Table 2.13: Acceptance criteria for physical and mechanical characteristics of BFRP rebar (Imperial Units)

			BFRP					
			FDOT 932-3/2017	AC454	ASTM D 7957	CAN/CSA S807	FIB Bulletin 40	GOST 31938 -2012
Test Method	Test Description	Unit	Criteria	Criteria	Criteria	Criteria	Criteria	Criteria
ASTM D 2584	Fiber Content	% wt.	n/a	n/a	n/a	TBD	n/a	n/a
ASTM D 570	Moist. Absorption short term @50 °C	%	n/a	n/a	n/a	TBD	n/a	n/a
ASTM D 570	Moist. Absorption long term @50 °C	%	n/a	n/a	n/a	TBD	n/a	n/a
ASTM D 7617	Min. Guaranteed Transverse Shear	ksi	n/a	n/a	n/a	TBD	n/a	n/a
ASTM D 4475	Horizontal Shear Stress	ksi	n/a	n/a	n/a	TBD	n/a	n/a
ACI440. 3 R,B.3	Bond-to-concrete strength	ksi	n/a	n/a	n/a	TBD	n/a	$\geqslant 1.74$

2.6 Required Chemical Durability of Rebar

The maximum strength reduction of rebars exposed to alkaline environment with a dead load is listed in Table 2.14.

Table 2.14: Acceptance criteria for chemical durability of rebar

		Reduction of strength after alkaline exposure with load					
		FDOT 932-3/2017	AC454	ASTM D 7957	CAN/CSA S807	FIB Bulletin 40	GOST 31938 -2012
Rebar Type	Unit	Criteria	Criteria	Criteria	Criteria	Criteria	Criteria
GFRP	%	$\leqslant 30$	$\leqslant 30$	$\leqslant 30$	$\leqslant 40$	n/a	$\leqslant 25$
BFRP	%	n/a	n/a	n/a	TBD	n/a	$\leqslant 25$

References

ACI Committee 440 (2007). *Report on Fiber-Reinforced Polymer (FRP) Reinforcement for Concrete Structures*, (440R). American Concrete Institute.

Alia, C., Biezma, M. V., Pinilla, P., Arenas, J. M., and Suárez, J. C. (2013). "Degradation in seawater of structural adhesives for hybrid fibre-metal laminated materials." *Advances in Materials Science and Engineering*, *2013*.

Alía, C., Jofre-Reche, J. A., Suárez, J. C., Arenas, J. M., and Martín-Martínez, J. M. (2015). "Influence of post-curing temperature on the structure, properties, and adhesion of vinyl ester adhesive." *Journal of Adhesion Science and Technology*, *29*(6), 518–531.

Aouf, C., Nouailhas, H., Fache, M., Caillol, S., Boutevin, B., and Fulcrand, H. (2013). "Multifunctionalization of gallic acid. synthesis of a novel bio-based epoxy resin." *European Polymer Journal*, *49*(6), 1185–1195.

Arias, J. P. M., Bernal, C., Vázquez, A., and Escobar, M. M. (2018). "Aging in water and in an alkaline medium of unsaturated polyester and epoxy resins: Experimental study and modeling." *Advances in Polymer Technology*, *37*(2), 450–460.

Aubourg, P., Crall, C., Hadley, J., Kaverman, R., and Miller, D. (1991). *Engineered Materials Handbook*, (Vol. 4). ASM International.

Bagherpour, S. (2012). (*Polyester*). InTech.

Baley, C., Busnel, F., Grohens, Y., and Sire, O. (2006). "Influence of chemical treatments on surface properties and adhesion of flax fibre–polyester resin." *Composites Part A: Applied Science and Manufacturing*, *37*(10), 1626–1637.

Banibayat, P. (2011). "Experimental investigation of the mechanical and creep rupture properties of basalt fiber reinforced polymer (bfrp) bars," Dissertation, The University of Akron.

Benmokrane, B., Ali, A. H., Mohamed, H. M., ElSafty, A., and Manalo, A. (2017). "Laboratory assessment and durability performance of vinyl-ester, polyester, and epoxy glass-frp bars for concrete structures." *Composites Part B: Engineering*, *114*, 163–174.

Benmokrane, B., Elgabbas, F., Ahmed, E. A., and Cousin, P. (2015). "Characterization and comparative durability study of glass/vinylester, basalt/vinylester, and basalt/epoxy frp bars." *Journal of Composites for Construction*, *19*(6), 04015008.

Benmokrane, B., Wang, P., Ton-That, T. M., Rahman, H., and Robert, J.-F. (2002). "Durability of glass fiber-reinforced polymer reinforcing bars in concrete environment." *Journal of Composites for Construction*, *6*(3), 143–153.

Best, M. G. (2003). *Igneous and metamorphic petrology*, (2nd Edition). Wiley-Blackwell.

Borges, S. G., Ferreira, C. A., Andrade, J. M., and Prevedello, A. L. (2015). "The influence of bath temperature on the properties of pultruded glass fiber reinforced rods." *Journal of Reinforced Plastics and Composites*, *34*(15), 1221–1230.

Carbas, R., Da Silva, L., Marques, E., and Lopes, A. (2013). "Effect of post-cure on the glass transition temperature and mechanical properties of epoxy adhesives." *Journal of Adhesion Science and Technology*, *27*(23), 2542–2557.

Cook, W. D., Simon, G. P., Burchill, P. J., Lau, M., and Fitch, T. J. (1997). "Curing kinetics and thermal properties of vinyl ester resins." *Journal of Applied Polymer Science*, *64*(4), 769–781.

Deák, T. and Czigány, T. (2009). "Chemical composition and mechanical properties of basalt and glass fibers: A comparison." *Textile Research Journal*, *79*(7), 645–651.

Dhé, P. (1923). *"Tipping crucible for basalt furnaces."* Patent 1,462,446, United States Patent Office.

Dodds, E. C. and Lawson, W. (1936). "Synthetic strogenic agents without the phenanthrene nucleus." *Nature*, *137*(3476), 996.

Dzhigiris, D., Makhova, M., Gorobinskaya, V., and Bombyr', L. (1983). "Continuous basalt fiber." *Glass and Ceramics*, *40*(9), 467–470.

Faruk, O., Tjong, J., and Sain, M. (2017). (*Lightweight and Sustainable Materials for Automotive Applications*). Tyler & Francis Group, LCC.

Fink, J. K. (2017). (*Reactive Polymers: fundamentals and applications: a concise guide to industrial polymers*). William Andrew.

Guo, F., Al-Saadi, S., Raman, R. S., and Zhao, X. (2018). "Durability of fiber reinforced polymer (frp) in simulated seawater sea sand concrete (swssc) environment." *Corrosion Science*, *141*, 1–13.

Huang, Y.-J. and Liang, C.-M. (1996). "Volume shrinkage characteristics in the cure of low-shrink unsaturated polyester resins." *Polymer*, *37*(3), 401–412.

Ipbüker, C., Nulk, H., Gulik, V., Biland, A., and Tkaczyk, A. H. (2014). "Radiation shielding properties of a novel cement–basalt mixture for nuclear energy applications." *Nuclear Engineering and Design*, *284*, 27–37.

Ivashchenko, E. (2009). "Sizing and finishing agents for basalt and glass fibers." *Theoretical Foundations of Chemical Engineering*, *43*(4), 511–516.

Jamshaid, H. and Mishra, R. (2016). "A green material from rock: basalt fiber — a review." *The Journal of The Textile Institute*, *107*(7), 923–937.

Johannesson, B., Sigfusson, T. I., Franzson, H., Erlendsson, Ö., Hardarson, B. S., Thorhallsson, E. R., Arnason, A. B., Azrague, K., Wiik, M. R. K., Vares, S., et al. (2017). (*GREENBAS: Sustainable Fibres from Basalt Mining*). Nordisk Ministerråd.

Joshi, S. C., Lam, Y., and Tun, U. W. (2003). "Improved cure optimization in pultrusion with pre-heating and die-cooler temperature." *Composites Part A*, *34*, 1151–1159.

Jung, T. and Subramanian, R. (1994). "Alkali resistance enhancement of basalt fibers by hydrated zirconia films formed by the sol-gel process." *Journal of materials research*, *9*(4), 1006–1013.

Kajorncheappunngam, S., Gupta, R. K., and GangaRao, H. V. (2002). "Effect of aging environment on degradation of glass-reinforced epoxy." *Journal of composites for construction*, *6*(1), 61–69.

King, M., Srinivasan, V., and Purushothaman, T. (2014). "Basalt fiber an ancient material for innovative and modern application." *Middle-East Journal of Scientific Research*, *22*(2), 308–312.

Kinkelaar, M., Wang, B., and Lee, L. J. (1994). "Shrinkage behaviour of low-profile unsaturated polyester resins." *Polymer*, *35*(14), 3011–3022.

Kochergin, A., Granovskaya, N., Kochergin, D., Savchenko, V., and Galimov, N. (2013). "Ways to supply gabbro-basalt raw materials to mineral fiber producers." *Glass and Ceramics*, *69*(11-12), 405–408.

Lipatov, Y. V., Gutnikov, S., Manylov, M., and Lazoryak, B. (2012). "Effect of zro 2 on the alkali resistance and mechanical properties of basalt fibers." *Inorganic materials*, *48*(7), 751–756.

Lipatov, Y. V., Gutnikov, S., Manylov, M., Zhukovskaya, E., and Lazoryak, B. (2015). "High alkali-resistant basalt fiber for reinforcing concrete." *Materials & Design*, *73*, 60–66.

McConnell, V. P. (2010). "Vinyl esters get radical in composite markets." *Reinforced Plastics*, *54*(6), 34–38.

Militkỳ, J., Kovačič, V., and Rubnerova, J. (2002). "Influence of thermal treatment on tensile failure of basalt fibers." *Engineering Fracture Mechanics*, *69*(9), 1025–1033.

Mingchao, W., Zuoguang, Z., Yubin, L., Min, L., and Zhijie, S. (2008). "Chemical durability and mechanical properties of alkali-proof basalt fiber and its reinforced epoxy composites." *Journal of Reinforced Plastics and Composites*, *27*(4), 393–407.

Morova, N. (2013). "Investigation of usability of basalt fibers in hot mix asphalt concrete." *Construction and Building Materials*, *47*, 175–180.

Morozov, N., Bakunov, V., Morozov, E., Aslanova, L., Granovskii, P., Prokshin, V., and Zemlyanitsyn, A. (2001). "Materials based on basalts from the european north of russia." *Glass and Ceramics*, *58*(3-4), 100–104.

Nanni, A., De Luca, A., and Jawaheri Zadeh, H. (2014). (*FRP Reinforced Concrete Structures – Theory, Design and Practice*). CRC Press.

Nasir, V., Karimipour, H., Taheri-Behrooz, F., and Shokrieh, M. (2012). "Corrosion behaviour and crack formation mechanism of basalt fibre in sulphuric acid." *Corrosion Science*, *64*, 1–7.

Nouranian, S., Lee, J., Torres, G., Lacy, T., Toghiani, H., and Pittman Jr, C. (2013). "Effects of moulding condition and curing atmosphere on the flexural properties of vinyl ester." *Polymers and Polymer Composites*, *21*(2), 61–64.

Novitskii, A. and Efremov, M. (2013). "Technological aspects of the suitability of rocks from different deposits for the production of continuous basalt fiber." *Glass and Ceramics*, *69*(11-12), 409–412.

Pavlovski, D., Mislavsky, B., and Antonov, A. (2007). "Cng cylinder manufacturers test basalt fibre." *REINFORCEDplastics*, 36–39.

Perevozchikova, B., Pisciotta, A., Osovetsky, B., Menshikov, E., and Kazymov, K. (2014). "Quality evaluation of the kuluevskaya basalt outcrop for the production of mineral fiber, southern urals, russia." *Energy procedia*, *59*, 309–314.

Pico, D., Wilms, C., Seide, G., and Gries, T. (2011). "Natural volcanic rock fibers." *Chemical Fibers International*, *61*(2), 90.

Pisciotta, A., Perevozchikov, B., Osovetsky, B., Menshikova, E., and Kazymov, K. (2015). "Quality assessment of melanocratic basalt for mineral fiber product, southern urals, russia." *Natural Resources Research*, *24*(3), 329–337.

Rybin, V., Utkin, A., and Baklanova, N. (2013). "Alkali resistance, microstructural and mechanical performance of zirconia-coated basalt fibers." *Cement and Concrete Research*, *53*, 1–8.

Rybin, V., Utkin, A., and Baklanova, N. (2016). "Corrosion of uncoated and oxide-coated basalt fibre in different alkaline media." *Corrosion Science*, *102*, 503–509.

Saadatmanesh, H., Tavakkolizadeh, M., and Mostofinejad, D. (2010). "Environmental effects on mechanical properties of wet lay-up fiber-reinforced polymer." *ACI materials journal*, *107*(3), 267.

Shokrieh, M., Nasir, V., and Karimipour, H. (2012). "A micromechanical study on longitudinal strength of fibrous composites exposed to acidic environment." *Materials & Design*, *35*, 394–403.

Singha, K. (2012). "A short review on basalt fiber." *International Journal of Textile Science*, *1*(4), 19–28.

Stekloplastics, D. (2014). "Stekloplastic visit to iceland." *Communication with Stekloplastics Boris Gromkov and Natalya Demenia with Birgir Jóhannesson*.

Tatarintseva, O. and Khodakova, N. (2010). "Obtaining basaltic continuous and staple fibers from rocks in krasnodar krai." *Glass and Ceramics*, *67*(5-6), 165–168.

Tatarintseva, O. and Khodakova, N. (2012). "Effect of production conditions of basalt glasses on their physicochemical properties and drawing temperature range of continuous fibers." *Glass physics and chemistry*, *38*(1), 89–95.

Tatarintseva, O., Khodakova, N., and Uglova, T. (2012a). "Dependence of the viscosity of basalt melts on the chemical composition of the initial mineral material." *Glass and ceramics*, *68*(9-10), 323–326.

Tatarintseva, O., Khodakova, N., and Uglova, T. (2012b). "Effect of iron oxides on the proneness of synthesized basaltic metals toward fiber formation." *Glass and Ceramics*, *69*(1-2), 71–74.

Toni Schneider, G. L. (2015). "Lipex gmbh, germany." *Communication with Toni Schneider, Gert Lichblau with Birgir Jóhannesson*.

Van Blaaderen, A., Van Geest, J., and Vrij, A. (1992). "Monodisperse colloidal silica spheres from tetraalkoxysilanes: particle formation and growth mechanism." *Journal of colloid and interface science*, *154*(2), 481–501.

Vasil'eva, A., Kychkin, A., Anan'eva, E., and Lebedev, M. (2014). "Investigation into the properties of basalt of the vasil'evskoe deposit in yakutia as the raw material for obtaining continuous fibers." *Theoretical foundations of chemical engineering*, *48*(5), 667–670.

Wei, B., Cao, H., and Song, S. (2010). "Tensile behavior contrast of basalt and glass fibers after chemical treatment." *Materials & Design*, *31*(9), 4244–4250.

Wei, B., Cao, H., and Song, S. (2011). "Surface modification and characterization of basalt fibers with hybrid sizings." *Composites Part A: Applied Science and Manufacturing*, *42*(1), 22–29.

Wei, B., Song, S., and Cao, H. (2011). "Strengthening of basalt fibers with nano-sio2–epoxy composite coating." *Materials & Design*, *32*(8-9), 4180–4186.

y de Caso, B. F. J., Matta, F., and Nanni, A. (2012). "Fiber reinforced cement-based composite system for concrete confinement." *Construction and Building Materials*, *32*, 55–65.

Ying, S. and Zhou, X. (2013). "Chemical and thermal resistance of basalt fiber in inclement environments." *Journal of Wuhan University of Technology-Mater. Sci. Ed.*, *28*(3), 560–565.

You, Y.-J., Kim, J.-H. J., Kim, S.-J., and Park, Y.-H. (2015). "Methods to enhance the guaranteed tensile strength of gfrp rebar to 900 mpa with general fiber volume fraction.." *Construction and Building Materials*, *75*, 54 – 62.

Zych, T. and Wojciech, K. (2012). "Study on the properties of cement mortars with basalt fibres." *Brittle Matrix Composites 10*, 155–166.